^{1}H-Detected, Gradient-Enhanced ^{15}N and ^{13}C NMR Experiments for the Measurement of Small Heteronuclear Coupling Constants and Isotopic Shifts

Gottfried Otting,[†] Barbara A. Messerle,*[,‡] and Linnea P. Soler[‡]

Contribution from the Department of Medical Biochemistry and Biophysics, Karolinska Institute, S-171 77 Stockholm, Sweden, and Department of Organic Chemistry, University of Sydney, Sydney NSW 2006, Australia

Received November 29, 1995[⊗]

Abstract: A suite of ^{1}H-detected, gradient-enhanced experiments is presented for the measurement of small ^{1}H−^{15}N and ^{13}C−^{15}N coupling constants in small organic compounds, where no protons are directly bound to the nitrogens. The experiments are based on modified HMQC pulse sequences and a novel gradient supported half-filter element. The experiments were applied to obtain a complete set of coupling constants in tris(1-pyrazolyl)methane (**1**), where 6% of the aromatic ring systems were doubly enriched with ^{15}N. The absolute sign of the ^{1}H−^{1}H, ^{1}H−^{15}N, ^{13}C−^{15}N, and ^{15}N−^{15}N coupling constants was determined by relating them to the sign of a one-bond ^{1}H−^{13}C coupling constant. The experiments also yield multiple bond ^{13}C/^{12}C isotope effects on the ^{15}N chemical shifts. The ^{1}H−^{15}N and ^{13}C−^{15}N coupling constants in **1** are non-uniform, with some of the short-range coupling constants smaller than the longer range coupling constants. In contrast, all one-bond ^{13}C/^{12}C isotope effects on the ^{15}N chemical shifts were observed to be significantly larger than the isotope effects mediated via two or more bonds. The one-bond isotope effect thus provides a valuable tool for assigning ^{15}N resonances in cases where coupling constant data yield ambiguous results.

Introduction

The measurement of coupling constants is an essential part of the characterization of the structure of organic and organometallic compounds by NMR spectroscopy. Both homonuclear and heteronuclear coupling constants are sensitive to the electronic structure of bonded atoms, and to the molecular geometry in terms of dihedral angles.[1,2] In organometallic compounds the magnitude of the coupling constants can provide information about the stereochemistry of metal complexes, as well as the oxidation state and coordination geometry of the central metal atom.[3−6] For metal phosphine complexes it has been established that the relative magnitude and sign of ^{31}P−^{31}P and ^{1}H−^{1}H coupling constants is characteristic of the relative position of the metal bound nuclei about the metal center, *e.g.* $^{2}J_{\mathrm{P-M-P(trans)}} > {}^{2}J_{\mathrm{P-M-P(cis)}}$ for six-coordinate iron(II) phosphine complexes, and also the metal center itself.[3−5] Less is known about the relative sign and size of coupling constants for metal complexes containing nitrogen donor ligands, or even the ligands themselves.

The metal centers in naturally occurring metalloenzymes are frequently coordinated by imidazole nitrogens. Using pyrazole as an imidazole analogue in the synthesis of metalloenzyme mimetics, a large number of metal complexes of poly(1-pyrazolyl)borate and poly(1-pyrazolyl)methane ligands have been synthesized.[7,8] Tris(1-pyrazolyl)borate complexes of Ir,[9] Rh,[10] and Re[11] have been shown to be reactive species which will insert into C−H bonds. Current efforts focus on polypyrazolylmethanes which are neutral compounds isosteric and isoelectronic with polypyrazolylborates.

The heteronuclear coupling constants ^{1}H−^{15}N and ^{13}C−^{15}N with the ^{15}N nuclei ligating the metal center are likely to contain information about the stereochemistry of the metal complexes. Yet, these coupling constants are difficult to measure routinely and accurately because of the rather low magnetic moment and low natural abundance of ^{15}N. Data on ^{13}C−^{15}N and ^{1}H−^{15}N coupling constants in pyrazole derivatives are scarce and mostly lack the sign of the coupling constants.[12,13] To alleviate the expense of ^{15}N labeling in establishing a data base of ^{1}H−^{15}N and ^{13}C−^{15}N coupling constants in metal complexes with nitrogen containing ligands, a strategy of low-level ^{15}N enrichment was adopted combined with NMR experiments developed for the sensitive detection of the coupling constants of interest.

Of the methods for the determination of small scalar coupling constants, two-dimensional experiments yielding E.COSY type multiplet patterns stand out for the ease with which the coupling constants can be read from the spectra.[14] E.COSY type multiplet patterns are observed whenever a passive spin, which is coupled to both spins involved in the cross peak, is left unaffected by the pulse sequence between the evolution time t_1 and the detection period t_2.[14−17] With the advent of self-shielded

* Address correspondence to this author.
[†] Karolinska Institute.
[‡] University of Sydney.
[⊗] Abstract published in *Advance ACS Abstracts,* May 1, 1996.

(1) Karplus, M. *J. Am. Chem. Soc.* **1963**, *85*, 2870−2871.
(2) Bystrov, V. F. *Prog. NMR Spectrosc.* **1976**, *10*, 41−81.
(3) Moore, D. S.; Robinson, S. D. *Chem. Soc. Rev.* **1983**, *12*, 415−452.
(4) Kaesz, H. D.; Saillant, R. B. *Chem. Rev.* **1972**, *72*, 231−281.
(5) Baker, M. V.; Field, L. D. *Inorg. Chem.* **1987**, *26*, 2010−2011.
(6) Bampos, N.; Field, L. D.; Messerle, B. A. *Organometallics* **1993**, *12*, 2529−2535.
(7) Trofimenko, S. *Chem. Rev.* **1993**, *93*, 943−980.
(8) Trofimenko, S. *Chem. Rev.* **1972**, *72*, 497−509.
(9) Tanke, R. S.; Crabtree, R. H. *Inorg. Chem.* **1989**, *28*, 3444−3447.
(10) Ghosh, C. K.; Graham, W. A. *J. Am. Chem. Soc.* **1987**, *109*, 4726−4727.
(11) Brown, S. N.; Mayer, J. M. *J. Am. Chem. Soc.* **1994**, *116*, 2219−2220.
(12) Fruchier, A.; Pellegrin, V.; Claramunt, R. M.; Elguero, *J. Org. Magn. Reson.* **1984**, *22*, 473−474.
(13) Hawkes, G. E.; Randall, E. W.; Elguero, J.; Marzin, C. J. *J. Chem. Soc., Perkin Trans. 2* **1976**, 1024−1027.
(14) Griesinger, C.; Sørensen, O. W.; Ernst, R. R. *J. Chem. Phys.* **1986**, *85*, 6837−6852.

S0002-7863(95)04017-0 CCC: $12.00

gradients,[18] previously difficult ^{1}H detected heteronuclear correlation experiments can be recorded routinely at natural isotopic abundance with a very low level of t_1 noise even when using short repetition times for small organic compounds with long relaxation times.[19] In the following, several gradient enhanced NMR pulse sequences using ^{1}H detection are presented which were designed to yield E.COSY-type multiplet patterns for the measurement of ^{1}H−^{15}N and ^{13}C−^{15}N coupling constants in tris(1-pyrazolyl)methane (**1**). The compound was doubly

(1)

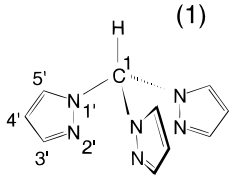

labeled with ^{15}N to a level of 6%. The experiments enable the determination of the absolute sign of the heteronuclear coupling constants by relating them to the sign of a one-bond ^{1}H−^{13}C coupling and yield the one bond and multiple bond ^{13}C/^{12}C isotope effects on the ^{15}N chemical shift. They are quite generally applicable to molecules with no or moderate ^{15}N enrichment and natural ^{13}C abundance and do not require that the nitrogen is bound to a proton.

Results

The ^{1}H NMR spectrum of **1** contains four ^{1}H resonances which were unambiguously assigned by a NOESY experiment with 1.5 s mixing time. The largest ^{1}H−^{1}H coupling constants observed are about 1.6 Hz between $H_{3'}$ and $H_{4'}$ and 2.5 Hz between $H_{4'}$ and $H_{5'}$ and were measured directly from the multiplet splitting observed in the 1D ^{1}H NMR spectrum. The chemical shifts of the two ^{15}N resonances were measured from a conventional ^{15}N HMQC experiment[20] correlating the proton signals via heteronuclear long-range couplings to the ^{15}N spins (data not shown). The resonances at 210.7 and 303.4 ppm were assigned to $N_{1'}$ and $N_{2'}$, respectively. This assignment was initially based on the empirical observation that pyrazol nitrogens with aliphatic substituents are at lower frequency in the ^{15}N NMR spectrum than those without substituent, in agreement with quantum mechanical calculations.[21] All subsequent ^{1}H−^{15}N correlation spectra were folded to obtain a good digital resolution in the indirectly detected frequency dimension with short recording times.

Measurement of ^{1}H−^{15}N Coupling Constants. Most of the ^{1}H−^{15}N coupling constants could be measured from a straightforward ^{15}N HMQC-45 experiment taking advantage of the special labeling pattern of compound **1**, where 6% of the nitrogen pairs in each pyrazolyl ring are *simultaneously* labeled with ^{15}N. Like in small flip angle COSY experiments,[16] the 45° pulse in the ^{15}N HMQC-45 experiment leaves passive ^{15}N spins which are coupled to the precessing ^{15}N spin mostly unaffected.[22] The resulting cross peak multiplets have an E.COSY type appearance with respect to the passive ^{15}N spin. Figure 1A shows the pulse sequence of the ^{15}N HMQC-45 experiment. Pulsed field gradients (PFG) are used to support the coherence order selection and suppress the signals from protons not coupled to ^{15}N. Phase sensitive data representations are obtained by recording echo and antiecho data.[26] The first two gradients are of opposite sign and symmetrically placed around a 180°(^{15}N) refocusing pulse. The effective evolution time for the ^{1}H−^{15}N coupling, Δ, is the same before and after t_1. The sequence δ-180°(^{15}N)−δ is inserted after the 90°(^{1}H) excitation pulse to refocus the ^{1}H chemical shifts at the start of data acquisition. In this way, all signals from refocused in-phase magnetization can be phased to absorption irrespective of the chemical shifts avoiding the long tails associated with dispersive in-phase magnetization. The tails from dispersive antiphase magnetization also present at the start of the acquisition time tend to be less important due to their partial cancellation by the antiphase multiplet fine structure.[27]

Figure 2A shows the ^{15}N HMQC-45 spectrum obtained with the pulse sequence of Figure 1A. The cross peaks are split in the F_1 dimension by the one-bond ^{15}N−^{15}N coupling constant (−13.0 Hz) and in F_2 by ^{1}H−^{15}N as well as ^{1}H−^{1}H couplings. The tilted appearance of the cross peaks is due to the passive ^{15}N spin which couples to the ^{15}N spin at the F_1 frequency of the cross peak and the ^{1}H spin at the F_2 frequency of the cross peak. Therefore, the relative displacement of the two multiplet components in the F_2 dimension, which are separated by the ^{15}N−^{15}N coupling in F_1, corresponds to the ^{1}H−^{15}N coupling constant between the detected proton spin and the ^{15}N spin at the *other* ^{15}N frequency in F_1. The small ^{1}H−^{15}N coupling constants are measured at the high resolution of the F_2 frequency axis. The tilt of the cross peaks relates the sign of the ^{1}H−^{15}N couplings to the sign of the ^{15}N−^{15}N coupling. Since the 180°(^{15}N) pulse between the first two gradients inverts both the active and passive ^{15}N spins, a positive tilt of the cross peaks as observed in Figure 2A, for example, for the cross peaks with $H_{3'}$, indicates that the ^{1}H−^{15}N coupling is of opposite sign as the ^{15}N−^{15}N coupling. The spectrum of Figure 2A yields six out of eight possible ^{15}N−^{1}H cross peaks and a corresponding number of ^{1}H−^{15}N coupling constants. Because of the large spread of J_{HN} values, the delay Δ could not be tuned to match $1/(2J_{HN})$ for all correlations simultaneously. For the Δ value chosen (90 ms), the ^{1}H−^{15}N coupling constants $J(H_{5'},N_{2'})$ and $J(H_{4'},N_{2'})$ are too small to lead to observable cross peaks in this experiment which prevents the measurement of the couplings $J(H_{5'},N_{1'})$ and $J(H_{4'},N_{1'})$.

A ^{1}H TOCSY with ^{15}N(ω_1) half-filter was recorded to measure those ^{1}H−^{15}N coupling constants which could not be measured from the spectrum of Figure 2A. The half-filter element proposed by Zerbe et al.[29] was supplemented by PFGs to support the selection of protons coupled to ^{15}N (Figure 1B). A 90°(^{15}N) pulse was inserted at the end of the ^{15}N(ω_1)-half-filter element to turn any unrefocused proton magnetization which is antiphase with respect to ^{15}N into unobservable multiple quantum coherence. In this way, the ^{1}H multiplet fine structure in F_1 is in-phase with respect to the ^{1}H−^{15}N couplings.

Figure 2B shows selected spectral regions from the ^{1}H TOCSY with gradient-supported ^{15}N(ω_1) half-filter recorded

(15) Aue, W. P.; Bartholdi, E.; Ernst, R. R. *J. Chem. Phys.* **1976**, *64*, 2229−2246.
(16) Bax, A.; Freeman, R. *J. Magn. Reson.* **1981**, *44*, 542−561.
(17) Neuhaus, D.; Wagner, G.; Vasák, M.; Kägi, J. H. R.; Wüthrich, K. *Eur. J. Biochem.* **1984**, *143*, 659−667.
(18) Hurd, R. E. *J. Magn. Reson.* **1990**, *87*, 422−428.
(19) Hurd, R. E.; John, B. K. *J. Magn. Reson.* **1991**, 648−653.
(20) Bax, A.; Griffey, R. H.; Hawkins, B. L. *J. Magn. Reson.* **1983**, *55*, 301−315.
(21) Stefaniak, L.; Roberts, J. D.; Witanowski, M.; Webb, G. A. *Org. Magn. Reson.* **1984**, *22*, 215−220.
(22) Schmidt, J. M.; Ernst, R. R.; Aimoto, S.; Kainosho, M. *J. Biomol. NMR* **1995**, *6*, 95−105.
(23) Wider, G.; Dötsch, V.; Wüthrich, K. *J. Magn. Reson. A* **1994**, *108*, 255−258.
(24) Weigelt, J.; Otting, G. *J. Magn. Reson. A* **1995**, *113*, 128−130.
(25) Marion, D.; Ikura, M.; Tschudin, R.; Bax, A. *J. Magn. Reson.* **1989**, *85*, 393−399.
(26) Davis, A. L.; Keeler, J.; Laue, E. D.; Moskau, D. *J. Magn. Reson.* **1992**, *98*, 207−216.
(27) Rance, M.; Sørensen, O. W.; Bodenhausen, G.; Wagner, G.; Ernst, R. R.; Wüthrich, K. *Biochem. Biophys. Res. Commun.* **1983**, *117*, 479−485.
(28) Bax, A.; Davis, D. G. *J. Magn. Reson.* **1986**, *65*, 355−360.
(29) Zerbe, O.; Welsh, J. H.; Robinson, J. A.; von Philipsborn, W. *J. Magn. Reson.* **1992**, *100*, 329−335.

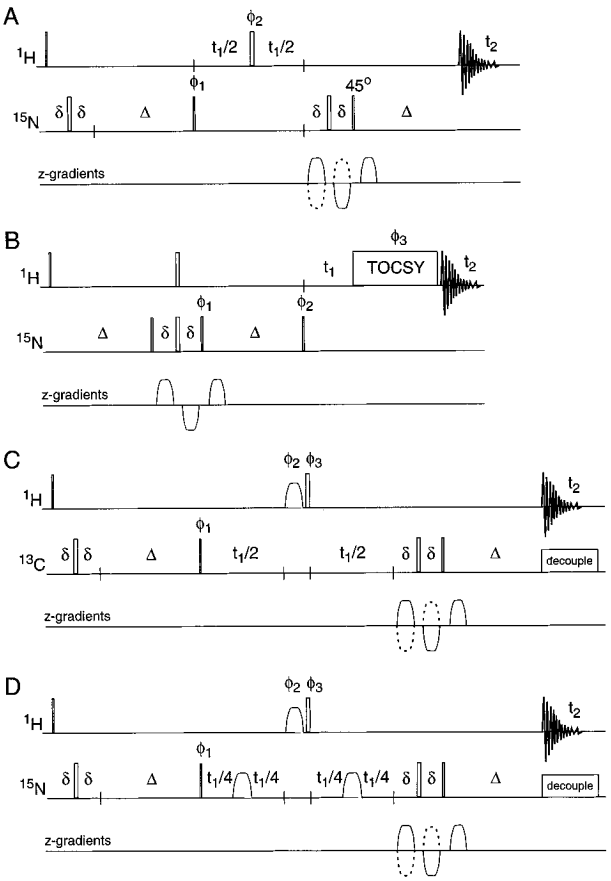

Figure 1. Experimental schemes used in the present work. Narrow and wide bars denote 90° and 180° pulses, respectively, except for the 45° pulse indicated in part A. Shaped pulses are symbolized by wider bars of non-rectangular shape and lower amplitude. SL identifies spin-lock pulses. All pulses are applied along the *x*-axis unless indicated differently. δ denotes the duration of a *z*-gradient including a short delay after the gradient for the recovery of the field homogeneity. All defocusing gradients are applied as a pair of gradients of opposite sign separated by a 180° pulse.[23,24] Phase-sensitive representations of the HMQC type spectra and improved signal-to-noise ratios are obtained by echo−antiecho selection (see experimental section). To support phase-sensitive representations, the sequence $\delta-180°-\delta$ is inserted in all HMQC type experiments before the heteronuclear *J*-coupling evolution period Δ which ensures symmetric defocusing and refocusing periods of the ^{1}H chemical shift evolution and of the heteronuclear couplings with the protons before and after the evolution time t_1. (A) ^{15}N HMQC-45: The experiment yields E.COSY type multiplet patterns with J_{NN} in the F_1 and J_{HN} in the F_2 dimensions. $\Delta = 1/(2J_{HN})$. Phase cycle: $\phi_1 = 4(x,-x)$; $\phi_2 = x,x,y,y,-x,-x,-y,-y$; receiver $= 2(x,-x,-x,x)$. (B) ^{1}H TOCSY with gradient supported ^{15}N(ω_1) half-filter: The experiment yields E.COSY type multiplet patterns with J_{HN} in both dimensions. $\Delta = 1/(2J_{HN})$. Phase cycle: $\phi_1 = 4(x,-x)$; $\phi_2 = 4(x),4(-x)$; $\phi_3 = 2(2(x),2(-x))$ added to the phases of all pulses of the mixing sequence; receiver $= 4(x,-x)$. Quadrature detection in F_1 is achieved by States-TPPI[25] applied to the phases of all proton pulses preceding t_1. (C) ^{13}C HMQC with selective refocusing pulse on one of the proton resonances. The experiment relates the sign of the J_{HH} couplings to the sign of the one-bond J_{HC} coupling of the selectively pulsed proton by providing E.COSY type multiplet patterns with $^1J_{HC}$ in F_1 and J_{HH} in F_2. $\Delta = 1/(2J_{HC})$. Phase cycle: $\phi_1 = 4(x,-x)$; $\phi_2 = 2(x,x,y,y)$; $\phi_3 = 4(x),4(y)$; receiver $= x,-x,-x,x,-x,x,x,-x$. (D) ^{15}N HMQC with selective refocusing pulse on one of the proton resonances. The experiment relates the sign of J_{HH} couplings to the sign of the J_{HN} couplings by providing E.COSY type multiplet patterns with J_{HN} in F_1 and J_{HH} in F_2. ^{15}N−^{15}N decoupling during t_1 is achieved by two selective ^{15}N inversion pulses applied at the frequency of the passive nitrogen spin. $\Delta = 1/(2J_{HN})$. Same phase cycle as in part C.

using the pulse sequence of Figure 1B. A section of the spectrum containing the diagonal peak of $H_{3'}$ and the related TOCSY cross peaks to the resonances of $H_{5'}$ and $H_{4'}$ is shown. Proton $H_{3'}$ has the largest coupling constants to the nitrogens, 13.0 and 8.8 Hz, giving rise to a well-resolved doublet of doublets on the diagonal. The TOCSY cross peaks with $H_{5'}$ and $H_{4'}$ display the same multiplet fine structure in the F_1 dimension. The relative shifts of the four components along the F_2 frequency axis reflect the ^{1}H−^{15}N coupling constants to the respective nitrogens which generate the multiplet of the diagonal peak of $H_{3'}$. It is apparent that the ^{15}N spin coupled to $H_{3'}$ with $J_{HN} = 8.8$ Hz gives rise to larger displacements of the multiplet components in the $H_{3'}-H_{5'}$ and $H_{3'}$-$H_{4'}$ cross peaks, while very small displacements in F_2 are observed for the J_{HN} coupling of 13.0 Hz. The small displacements correspond to the small coupling constants $J(H_{5'},N_{2'})$ and $J(H_{4'},N_{2'})$ measured in Figure 2A. The larger displacements correspond to the coupling constants $J(H_{5'},N_{1'})$ and $J(H_{4'},N_{1'})$. The positive tilt of the cross peaks indicates that the sign of the ^{1}H−^{15}N couplings is the same for both ^{1}H spins involved in the cross peaks.[30]

Determination of the Absolute Sign of ^{1}H−^{15}N and ^{15}N−^{15}N Coupling Constants. The absolute signs of the ^{1}H−^{15}N coupling constants are readily determined by relating them to the known sign of a one-bond ^{1}H−^{13}C coupling[31] in an E.COSY type experiment. Because of the low abundance of ^{15}N and ^{13}C, the direct correlation of ^{1}H−^{15}N and ^{1}H−^{13}C couplings in a single experiment is rather insensitive. Therefore, the better alternative is to determine first the sign of a selected ^{1}H−^{1}H coupling with respect to $^1J(^1H,^{13}C)$ and to relate in a second step the sign of $J(^1H,^{15}N)$ to the sign of the ^{1}H−^{1}H coupling constant. Figure 1C shows the pulse sequence used to relate the sign of the ^{1}H−^{1}H couplings $J(H_{4'},H_{3'})$ and $J(H_{4'},H_{5'})$ to the sign of the one-bond coupling $^1J(H_{4'},C_{4'})$. The experiment is based on a ^{13}C HMQC sequence supplemented by a selective 180° inversion pulse applied to the $H_{4'}$ resonance. The combined effect of the selective and the following nonselective inversion pulses is a 360° rotation of the $H_{4'}$ spin so that $H_{4'}$ remains effectively untouched during t_1 and t_2, and the time in between. As a result, the multiple bond correlations at the F_1 chemical shift of the $C_{4'}$ resonance assume E.COSY type appearances, with their multiplet components displaced by $^1J(H_{4'},C_{4'})$ in the F_1 dimension and $J(H_{4'},H_{det})$ in F_2, where H_{det} denotes the detected proton spin (Figure 2C). The positive tilt observed for the multiplet components of the $C_{4'}-H_{3'}$ and $C_{4'}-H_{5'}$ cross peaks indicates that the signs of $J(H_{4'},H_{3'})$ and $J(H_{4'},H_{5'})$ are the same as the sign of $^1J(H_{4'},C_{4'})$.

Once the sign of a J_{HH} coupling has been measured in relation to a one-bond J_{HC} coupling, the relative sign of J_{HN} with respect to J_{HH} can be determined by the ^{15}N HMQC type pulse sequence shown in Figure 1D. The sequence uses a selective 180° inversion pulse applied to the same proton resonance as the pulse sequence of Figure 1C. Selective 180°(^{15}N) inversion pulses applied to the passive ^{15}N spin simplify the multiplet pattern in F_1 by refocusing the J_{NN} coupling and facilitate the spectral interpretation. Two selective ^{15}N inversion pulses are required, because a single selective ^{15}N inversion pulse in the middle of t_1 would reintroduce the J-coupling between the refocused protons and the selectively pulsed ^{15}N spin during t_1. Figure 2D shows the spectral region containing the cross peaks $N_{1'}-H_{3'}$ and $N_{1'}-H_{5'}$. The cross peaks are split in the F_1 dimension by $J(H_{4'},N_{1'})$ and in F_2 by the couplings $J(H_{3'},H_{4'})$ and $J(H_{5'},H_{4'})$, respectively. The positive tilt of the cross peaks indicates that for these couplings J_{HN} and J_{HH} have the same sign.

The abovementioned experiments yield the absolute sign of $^1J(N_{1'},N_{2'})$ in **1**. Because $^1J(H_{4'},C_{4'})$ is positive,[31] the experiment

(30) Montelione, G. T.; Winkler, M. E.; Rauenbuehler, P.; Wagner, G. *J. Magn. Reson.* **1989**, *82*, 198−204.
(31) Kowalewski, J. *Prog. NMR Spectrosc.* **1977**, *11*, 1−78.

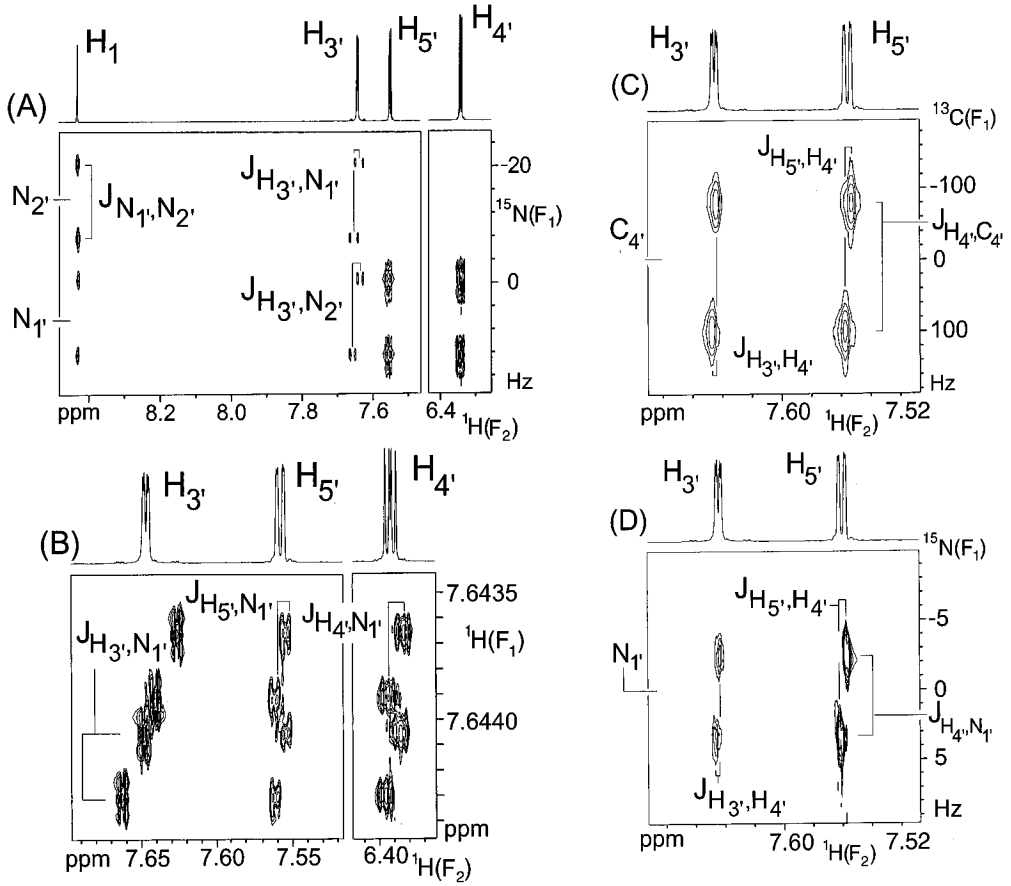

Figure 2. Selected spectral regions from the HMQC spectra of a 200 mM solution of **1** in $CDCl_3$ at 25 °C in a 5 mm sample tube using the pulse sequences of Figure 1. Positive and negative levels are plotted without distinction. The 1D spectrum of **1** is plotted at the top of each spectrum. (A) ^{15}N HMQC-45: $\Delta = 90$ ms, $t_{1max} = 576$ ms, 2 scans/FID, total recording time 7 min. For improved spectral representation, magnitude data were calculated in the F_2 dimension after a phase sensitive 2D Fourier transform. Each cross peak consists of two main components separated by J_{NN} in F_1 and J_{HN} in F_2, where J_{HN} is the coupling constant between the detected proton resonance and the passive ^{15}N spin which is *not* at the F_1 frequency of the cross peak. (B) ^{1}H TOCSY with gradient-supported ^{15}N(ω_1) half-filter. $\Delta = 75$ ms, TOCSY mixing time (MLEV-17)[28] 100 ms, $t_{1max} = 420$ ms, 8 scans/FID, total recording time 1 h. The diagonal peak of $H_{3'}$ is shown together with its cross peaks to $H_{5'}$ and $H_{4'}$. The four main multiplet components of $H_{3'}$ reflect its relatively large J_{HN} couplings to both ^{15}N spins. The J_{HN} couplings of $H_{5'}$ and $H_{4'}$ can be read from the displacements of the four multiplet components of the $H_{3'}-H_{5'}$ and $H_{3'}-H_{4'}$ cross peaks in the F_2 dimension. Magnitude data were calculated in the F_2 dimension after phase-sensitive Fourier transform. (C) ^{13}C HMQC with selective refocusing pulse on the $H_{4'}$ resonance. $\Delta = 50$ ms, $t_{1max} = 29$ ms, 2 scans/FID, total recording time 12 min. The cross peaks $C_{4'}-H_{3'}$ and $C_{4'}-H_{5'}$ are shown. The cross peaks are split in F_1 by $^1J(H_{4'},C_{4'})$ and in F_2 by $J(H_{4'},H_{3'})$ and $J(H_{4'},H_{5'})$, respectively. (D) ^{15}N HMQC with selective refocusing pulse on the $H_{4'}$ resonance. $\Delta = 90$ ms, $t_{1max} = 384$ ms, 2 scans/FID, total recording time 7 min. The cross peaks $N_{1'}-H_{3'}$ and $N_{1'}-H_{5'}$ are shown. The cross peaks are split in F_1 by $J(H_{4'},N_{1'})$ and in F_2 by $J(H_{4'},H_{3'})$ and $J(H_{4'},H_{5'})$, respectively.

of Figure 2C shows that $J(H_{4'},H_{3'})$ is positive; because $J(H_{4'},H_{3'})$ is positive, the experiment of Figure 2D shows that $J(H_{4'},N_{1'})$ is positive and thus, by virtue of the experiment of Figure 2A, $^1J(N_{1'},N_{2'})$ is negative in accordance with literature.[32,33]

Measurement of ^{13}C−^{15}N Coupling Constants and ^{12}C/^{13}C Isotope Effects on the ^{15}N Chemical Shifts. To explore the possibility of assigning the ^{15}N resonances in **1** via one bond J_{CN} couplings and/or ^{13}C/^{12}C isotope effects on the ^{15}N chemical shifts, novel pulse sequences were developed which yield E.COSY type multiplet patterns relating the J_{CN} coupling constants to the one bond J_{HC} couplings. Figure 3 shows the pulse sequences used. The sequences are based on ^{15}N HMQC experiments with the ^{13}C satellites of the proton signals. Since the ^{13}C spins are not pulsed either during the evolution time or during the detection period or between the two, E.COSY type multiplet patterns are obtained with respect to the ^{13}C spins, where the multiplet components are separated by the one-bond J_{HC} coupling constant of the detected proton spins in the F_2 dimension and by the J_{CN} coupling of the indirectly detected ^{15}N spin in the F_1 dimension. A positive tilt of the cross peaks indicates that the sign of the J_{CN} coupling constant is the same as for the J_{HC} coupling. The magnetization from the ^{13}C-bound protons is selected by a ^{13}C half-filter, where the half-filter element ends with a spin-lock purge pulse of about 2-ms duration to suppress the signals from ^{12}C-bound protons.[34] The selection of ^{13}C-bound protons is further supported by the phase cycle of the phase ϕ_1 yielding effective 0° and 180° pulses together with the preceding 90°(^{13}C) pulse. The pulse sequences of Figure 3 employ selective 180°(^{15}N) inversion pulses to enhance the sensitivity by refocusing passive ^{1}H−^{15}N and ^{15}N−^{15}N couplings during the J-evolution delay Δ and during t_1, respectively. The use of the additional selective pulses improved the sensitivity of the observed ^{1}H−^{15}N correlations by more than two-fold over experiments performed without the selective pulses. The improved resolution and the sensitivity advantage more than outweighs the disadvantage that correlations with only a single ^{15}N resonance can be observed at a time in the presence of the selective 180°(^{15}N) pulses.

Figures 4A and 4C show the spectral regions from two ^{15}N HMQC experiments with ^{13}C half-filter. The spectra were

(32) Berkhoudt, T.; Jakobsen, H. J. *J. Magn. Reson.* **1982**, *50*, 323−327.

(33) Kuroda, Y.; Fujiwara, Y.; Matsushita, K. *J. Chem. Soc., Perkin Trans. 2* **1985**, 1533−1536.

(34) Otting, G.; Wüthrich, K. *Q. Rev. Biophys.* **1990**, *23*, 39−96.

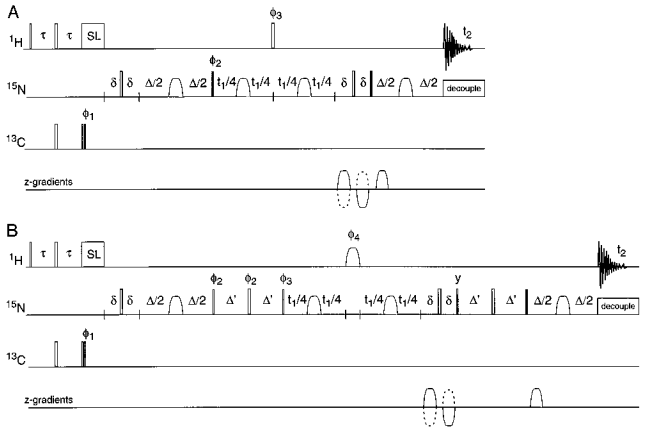

Figure 3. (A) ^{15}N HMQC with ^{13}C half-filter. The experiment correlates ^{13}C-bound protons to ^{15}N spins providing E.COSY type multiplet patterns with J_{CN} in F_1 and J_{HC} in F_2. ^{13}C/^{12}C isotope effects on the ^{15}N chemical shifts are obtained by comparison of the observed ^{15}N chemical shifts with the ^{15}N chemical shifts measured by a related pulse sequence, where the ^{13}C half-filter is replaced by a 90°(^{1}H) pulse with the phase ϕ_1. To enhance the sensitivity and resolution, selective inversion pulses are applied to one of the two ^{15}N spins during the delays Δ and t_1. The experiment yields the correlations to the ^{15}N spin not affected by the selective pulses. The correlations to the second ^{15}N spin are obtained in a second spectrum recorded with the selective pulses applied to the first ^{15}N resonance. $\tau = 1/(4J_{HC})$, $\Delta = 1/(2J_{HN})$. δ = duration for a pulsed field gradient. Phase cycle: $\phi_1 = 4(x,x,-x,-x)$; $\phi_2 = 8(x,-x)$; $\phi_3 = 4(x),4(y),4(-x),4(-y)$; receiver = $2(x,-x,-x,x,-x,x,x,-x)$. (B) ^{15}N HMQC with ^{13}C half-filter and ^{15}N−^{15}N relay. The experiment yields ^{15}N−^{1}H cross peaks with the same E.COSY type appearance as the sequence in (A) enabling the measurement of sign and size of J_{CN} couplings. The desired ^{1}H−^{15}N coherence during t_1 is established through ^{1}H−^{15}N coherence with another ^{15}N spin and a ^{15}N−^{15}N relay step. After the evolution time t_1, the magnetization is refocused following the same pathway in reverse. To enhance the sensitivity and resolution of correlations with nitrogen 1, selective inversion pulses are applied to nitrogen 1 during Δ and to nitrogen 2 during t_1. ^{1}H−^{1}H decoupling during t_1 is achieved by replacing the nonselective 180°(^{1}H) pulse of the ^{15}N HMQC schemes in Figures 1 and 3A by a selective proton refocusing pulse acting on the ^{1}H spins involved in the desired ^{15}N−^{1}H correlation. As in part A, ^{13}C/^{12}C isotope effects on the ^{15}N chemical shifts are obtained by comparison of the observed ^{15}N chemical shifts with the ^{15}N chemical shifts measured by a related pulse sequence, where the ^{13}C half-filter is replaced by a 90°(^{1}H) pulse with the phase ϕ_1. $\tau = 1/(4J_{HC})$, $\Delta = 1/(2J_{HN})$, $\Delta' = 1/(4J_{NN})$. Phase cycle: $\phi_1 = 4(x,x,-x,-x)$; $\phi_2 = 8(x,-x)$; $\phi_3 = 8(y,-y)$; $\phi_4 = 4(x),4(y),4(-x),4(-y)$; receiver = $2(x,-x,-x,x,-x,x,x,-x)$.

recorded using the pulse sequence of Figure 3A with the selective 180°(^{15}N) pulses applied to either $N_{2'}$ (Figure 4A) or $N_{1'}$ (Figure 4C). Seven out of eight possible correlations are observed showing the expected E.COSY type multiplet fine structure. Because of the large one-bond J_{HC} couplings, the cross peaks are well separated from the t_1 noise bands at the F_2 chemical shifts of the incompletely suppressed signals from ^{12}C-bound protons. Reference spectra recorded with identical parameters but without ^{13}C half-filter are plotted in Figures 4B and 4C below the corresponding spectra recorded with ^{13}C-half-filter. The ^{15}N−^{1}H cross peaks in the reference spectra are with ^{12}C-bound protons. The ^{15}N chemical shifts observed in the F_1 dimension of the spectra recorded with ^{13}C half-filter (Figures 4A and 4C) deviate from the chemical shifts observed in the corresponding reference spectra (Figures 4B and 4D) because of ^{13}C/^{12}C isotope effects on the ^{15}N chemical shifts.

The experiment of Figure 3A enables the measurement of J_{CN} coupling constants only, if the ^{13}C spin is bound to a proton with resolved J_{HN} coupling to the ^{15}N spin of interest. Since the coupling $J(H_{5'},N_{2'})$ is as small as −0.1 Hz, the corresponding ^{15}N−^{1}H cross peak could not be detected in the experiment of

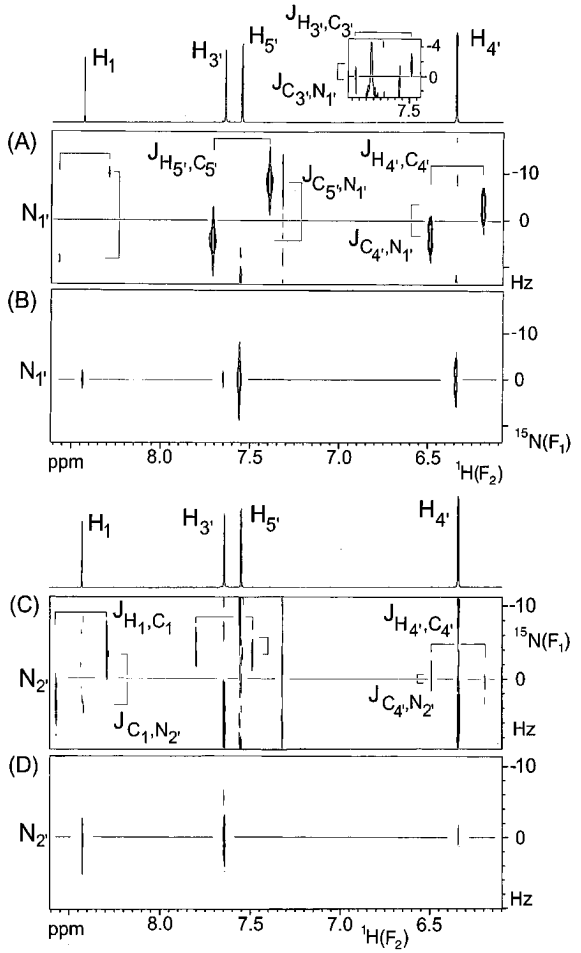

Figure 4. Selected spectral regions from ^{15}N HMQC spectra with ^{13}C half-filter recorded with the pulse sequence of Figure 3A. The cross peaks are antiphase with respect to the J_{HC} coupling. Positive and negative levels were plotted without distinction. The multiplet components are displaced by the coupling constants J_{CN} and J_{HC} in the F_1 and F_2 dimension, respectively. The horizontal line indicates the ^{15}N chemical shift from the reference spectrum recorded without ^{13}C half-filter. The cross peaks are displaced from the reference line by the ^{13}C/^{12}C isotope effects on the ^{15}N chemical shifts. (A) ^{15}N HMQC with ^{13}C half-filter. The selective inversion pulses (Figure 3A) were applied at the frequency of $N_{2'}$. The insert shows the cross peak $N_{1'}$−$H_{3'}$ which is visible only at lower plot levels. $\tau = 1.35$ ms, $\Delta = 90$ ms, $t_{1max} = 576$ ms, 128 scans/FID, total experimental time 9.5 h. (B) Reference spectrum for part A recorded under identical conditions with a 90°(^{1}H) pulse instead of the ^{13}C half-filter element. Two scans/FID, total recording time about 9 min. (C) Same as part A, except that the selective inversion pulses (Figure 3A) were applied at the frequency of $N_{1'}$. (D) Reference spectrum for part C recorded with a 90°(^{1}H) pulse replacing the ^{13}C half-filter element in Figure 3A.

Figure 4C. To obtain the missing correlation $N_{2'}$-$H_{5'}$ in an experiment suitable for the determination of the coupling constant $J(C_{5'},N_{2'})$, the coherence between $H_{5'}$ and $N_{2'}$ was created by evolving antiphase coherence between $H_{5'}$ and $N_{1'}$ ($J(H_{5'},N_{1'}) = 4.5$ Hz), followed by a ^{15}N−^{15}N relay step from $N_{1'}$ to $N_{2'}$. After frequency labeling during t_1, the coherence was refocused by a ^{15}N−^{15}N relay step from $N_{2'}$ to $N_{1'}$ and refocusing of the coherence between $H_{5'}$ and $N_{1'}$. Finally, the spin $H_{5'}$ was detected. Together with a ^{13}C half-filter, the experiment yields cross peaks of identical appearance as the pulse sequence of Figure 3A. A reference spectrum without ^{13}C satellite selection yields the ^{15}N chemical shifts of the correlations with ^{12}C-bound protons. The pulse sequence is shown in Figure 3B. Selective 180°(^{15}N) inversion pulses were applied on the spin $N_{2'}$ during the delays Δ and on $N_{1'}$ during t_1 to enhance the sensitivity and resolution of the desired

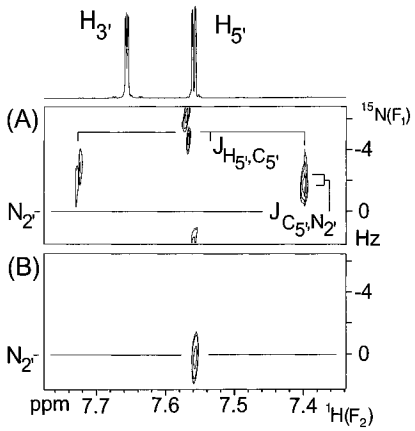

Figure 5. (A) ^{15}N HMQC with ^{13}C half-filter and ^{15}N−^{15}N relay recorded with the pulse sequence of Figure 3B. The selective ^{15}N inversion pulses during Δ and t_1 were applied to $N_{2'}$ and $N_{1'}$, respectively. The selective 180°(^{1}H) refocusing pulse acted on all resonances except $H_{4'}$. The two main multiplet components of the cross peak are displaced by $J(C_{5'},N_{2'})$ in F_1 and $J(H_{5'},C_{5'})$ in F_2. The horizontal line indicates the ^{15}N chemical shift from the reference spectrum. The cross peak is displaced from the reference line by the ^{13}C/^{12}C isotope effect on the ^{15}N chemical shift. τ = 1.35 ms, Δ = 110 ms, Δ' = 19 ms, t_{1max} = 576 ms, 256 scans/FID, total experimental time 20 h. (B) Reference spectrum for part A recorded with a 90°(^{1}H) pulse instead of the ^{13}C half-filter element. Two scans/FID, 10 min total recording time.

$N_{2'}$-$H_{5'}$ cross peak. With the high resolution necessary for the measurement of small ^{13}C−^{15}N coupling constants in the F_1 frequency dimension, small ^{1}H−^{1}H couplings evolving during the evolution time t_1 would be a major cause for line broadening (see, *e.g.*, the cross peaks $N_{1'}$-$H_{5'}$ and $N_{1'}$-$H_{4'}$ in Figure 4A). To improve the resolution and sensitivity of the $N_{2'}$-$H_{5'}$ cross peak, the coupling $J(H_{4'},H_{5'})$ was refocused by a semiselective 180°(^{1}H) refocusing pulse in the middle of t_1, which acted on all protons except for proton $H_{4'}$. Refocusing of the couplings between $H_{5'}$ and the other protons was not attempted, since none of these couplings is larger than 1.6 Hz and a more selective inversion pulse would have had to be much longer.

Figure 5A shows the cross peak $N_{2'}$-$H_{5'}$ in the ^{15}N HMQC experiment with ^{13}C half-filter and ^{15}N−^{15}N relay recorded with the pulse sequence of Figure 3B. The reference spectrum recorded without ^{13}C half-filter is plotted below (Figure 5B). The negative tilt observed for the two ^{13}C satellites indicates that the sign of the coupling constant J_{CN} is the opposite as for the one-bond coupling J_{HC}.

The measurements with partially ^{15}N labeled compound **1** cannot distinguish between couplings within the same pyrazolyl ring or between two nuclei located in different pyrazolyl rings across the methine bridge. Therefore, a sample of 99% ^{15}N enriched compound **1** was prepared and a conventional ^{13}C HSQC spectrum[35,36] recorded. Since ^{15}N nuclei are passive spins in this experiment, E.COSY type multiplet patterns were obtained with the ^{13}C−^{15}N couplings in the F_1 dimension and the ^{1}H−^{15}N couplings in the F_2 dimension. With a single exception, the observed cross peaks showed no multiplicities beyond those expected for the couplings measured with the 6% ^{15}N labeled sample. The exception is $C_{5'}$ which showed a line width of 1.6 Hz in the F_1 dimension while all other ^{13}C resonances had a line width of 0.8 Hz. This indicates unresolved ^{13}C−^{15}N couplings of the order of 0.4 Hz between $C_{5'}$ and the ^{15}N resonances in the other two pyrazolyl rings. Similarly, no further ^{1}H−^{15}N couplings were resolved in the ^{1}H multiplet fine-structures. The ^{1}H−^{15}N and ^{13}C−^{15}N coupling constants measured from the ^{13}C HSQC spectrum of the 100% ^{15}N labeled sample agreed within the digital resolution with the coupling constants obtained independently from the spectra recorded with the 6% ^{15}N enriched sample (Figures 2, 4, and 5). The only exception was $J(C_{4'},N_{2'})$, which was measured as −1.0 Hz from the experiment of Figure 4C, but was found to be −2.3 Hz in the ^{13}C HSQC experiment. The reason for the discrepancy is probably the low signal-to-noise ratio obtained for the $N_{2'}$−$H_{4'}$ cross peak in the experiment of Figure 4C.

Discussion

All coupling constant and isotope shift data obtained here were measured from high-resolution ^{1}H detected 2D NMR experiments, where the information is encoded in E.COSY type cross peak multiplets. ^{1}H−^{15}N coupling constants are read from the displacement of cross peak components in the F_2 dimension. ^{15}N−^{15}N and ^{13}C−^{15}N coupling constants cannot be read from the detected proton signals and therefore have to be measured in the F_1 frequency dimension. High digital resolution in the F_1 dimension was readily obtained by folding the spectra. With the resulting large time increments between subsequent t_1 data points, the total recording time per spectrum could be kept as short as a few minutes. In addition, phase correction of the spectra in the F_1 dimension was straightforward even in the presence of selective pulses in the t_1 evolution time which are a few milliseconds long and delay the initial t_1 sampling point.

With two exceptions, the experiments of Figures 1 and 3 are also suitable for the measurement of heteronuclear coupling constants in compounds containing single nitrogens. The exceptions are the experiments of Figures 1A and 3B which depend on the presence of two ^{15}N spins linked by a resolved ^{15}N−^{15}N coupling constant.

The accuracy of the measured coupling constants is mainly determined by the digital resolution. In principle, the coupling constants measured from E.COSY type multiplet patterns tend to be biased systematically to small values because antiphase coherence with respect to a passive spin relaxes more rapidly than in-phase magnetization.[30] Yet, this relaxation effect becomes important only for larger molecules with T_1 relaxation times comparable to the duration of the pulse sequence.

Figure 6 summarizes the ^{1}H−^{15}N, ^{15}N−^{15}N, and ^{13}C−^{15}N coupling constants together with the ^{13}C/^{12}C isotope effects on the ^{15}N chemical shift measured for **1**. There is a remarkable spread among the short-range coupling constants, with $^2J_{HN}$ ranging from −1.2 to 13.0 Hz and $^1J_{CN}$ ranging from −0.5 to 18.0 Hz. Yet, except for H_1, two-bond J_{HN} couplings are larger than three-bond J_{HN} couplings with the same proton spin. Except for $C_{3'}$, one-bond J_{CN} couplings are larger than two-bond J_{CN} couplings with the same carbon spin. Interestingly, all J_{CN} couplings within the pyrazol ring are positive with $N_{1'}$ but negative with $N_{2'}$. While the magnitudes of the couplings agree closely with literature data,[12,13] the spread in size prohibits their use for assigning the ^{15}N resonances, when **1** is bound as a ligand in metal complexes. For example, a heteronuclear INADEQUATE type experiment[37] attempting to pick ^{13}C−^{15}N connectivities via presumably large one-bond ^{13}C−^{15}N couplings would fail totally in the spin system represented by **1**. In this situation, the ^{13}C/^{12}C isotope effects on the ^{15}N chemical shift turn out to be the safest way of assigning the ^{15}N resonances, since the one-bond effects are always clearly larger than the multiple bond effects (Figure 6C).

(35) Bodenhausen, G.; Ruben, D. *J. Chem. Phys. Lett.* **1980**, *69*, 185−189.
(36) Otting, G.; Wüthrich, K. *J. Magn. Reson.* **1986**, *76*, 569−574.
(37) Bax, A.; Freeman, R.; Kempsell, S. P. *J. Am. Chem. Soc.* **1981**, *103*, 2102−2105.

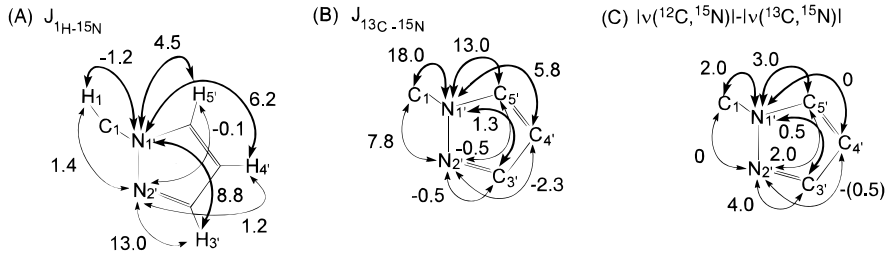

Figure 6. Overview over the coupling constants $^1H-^{15}N$ (A) and $^{13}C-^{15}N$ (B) and the $^{13}C/^{12}C$ isotope effects on the ^{15}N chemical shifts (C) observed in **1**. All values given in Hz. Some coupling constants were measured but not indicated in the figure: $^1J(^{15}N,^{15}N) = -13.0$ Hz, $^3J(H_{3'},H_{4'}) = 1.6$ Hz, $^3J(H_{4'},H_{5'}) = 2.5$ Hz. The error resulting from the limiting digital resolution in the F_1 and F_2 dimensions is ± 0.5 Hz for $^{15}N-^{15}N$, $^{13}C-^{15}N$ coupling constants and $^{13}C/^{12}C$ isotope effects, and ± 0.1 Hz for $^1H-^{15}N$ coupling constants. The isotope shift value in brackets is uncertain because of the low signal−to−noise ratio of the corresponding $N_{2'}-H_{4'}$ cross peak in Figure 4C.

Conclusion

The level of ^{15}N labeling of the compound and the concentration of the sample yielded unacceptable signal-to-noise ratios when attempting to record a 1D ^{15}N spectrum with direct ^{15}N detection using 12 h of measurement time. Therefore, ^1H detection was a prerequisite for the measurement of the data presented here. As demonstrated earlier, the use of gradients suppresses t_1 noise from protons not correlated to heteronuclei in spectra recorded at natural isotopic abundance.[19,26] The examples shown here demonstrate that with the help of gradients and a spin-lock purge pulse the measurement of $^{13}C-^{15}N$ coupling constants is possible at natural ^{13}C isotope abundance and ^{15}N enrichment at a level of only 6%. Clearly, the spectral quality would be sufficient to measure $^{13}C-^{15}N$ coupling constants also without any isotope enrichment, since overlap of the desired cross peaks with the most intense residual t_1 noise bands is avoided by detecting the ^{13}C satellites. To date, few data are available on multiple-bond $^{13}C-^{15}N$ coupling constants in organic molecules. Usually, the absolute signs of the couplings are left undetermined. There are virtually no data on $^{13}C/^{12}C$ isotope effects on ^{15}N chemical shifts. With the experimental schemes presented here, the measurement of these parameters becomes possible without taking recourse to expensive isotope enrichment. On this basis, the efficient buildup of a data base with heteronuclear coupling constants and isotope effects can be envisaged.

Experimental Section

NMR Experiments. Experimental parameters pertinent to all experiments were as follows: 600-MHz ^1H frequency, $t_{2max} = 1.3$ s, total relaxation delay between two scans 2.3 s, GARP decoupling[38] during data acquisition, and Bruker DMX-600 NMR spectrometer equipped with a triple-resonance probehead with self-shielded gradients. The gradient pulses used were "semi-sine" shaped, where each shape is represented by a histogram of 200 points with a sine-shaped rise over 32 points followed by a plateau of 136 points and a sine-shaped decay of 32 points.[24] All gradients were applied with a duration of 1 ms and at least a 200 μs recovery delay after each gradient resulting in $\delta = 1.2$ ms. For each of the HMQC type spectra, two FIDs corresponding to N and P type signals were recorded using gradient strengths of 11, −11, 2.23 G/cm and −11, 11, 2.23 G/cm, respectively, in the $^1H-^{15}N$ correlation experiments, and 11, −11, 5.54 G/cm and −11, 11, 5.54 G/cm for the N and P type FIDs in the $^1H-^{13}C$ correlation experiment. The time-domain data were combined to yield phase sensitive data representations.[39−41] G^3 pulse cascades[42] of 4.6-ms duration were used for all selective 180° inversion and refocussing pulses. All spectra were folded in the F_1 dimension to reduce the total recording time.

Synthesis of Tris(1-pyrazolyl)methane (1). The tridentate ligand (doubly labeled to 6% with ^{15}N) was synthesized using a mixture of unlabeled and 99% labeled ^{15}N pyrazole.

(a) Synthesis of 99% ^{15}N Pyrazole.[43] Ethanol (35 mL) and water (55 mL) were added to 99% ^{15}N-labeled hydrazine sulfate (2.14 g, 16 mmol) and the solution was stirred and heated at 75 °C for 1.5 h until the hydrazine fully dissolved. Malonaldehyde bis(dimethylacetal) (2.7 g, 16.4 mmol) was added dropwise and the solution was stirred and heated at 75 °C for 2 h. It was then stirred for 24 h at room temperature. The ethanol was removed under reduced pressure and the solution was neutralized with $CaCO_3$. After addition of water the solution was filtered through celite. The eluant was extracted with ether (2 × 25 mL, 25 × 10 mL), and the ether solution was dried over K_2CO_3 and filtered again through celite. The volume of ether was reduced by distillation and long needle-like crystals of 99% ^{15}N pyrazole were formed (1.12 g, yield: 96.3%).

(b) Synthesis of 6% ^{15}N-Labeled Tris(1-pyrazolyl)methane (1).[44] Chloroform (50 mL) was added to a mixture of 99% ^{15}N pyrazole (0.11 g, 1.58 mmol), unlabeled pyrazole (1.70 g, 30 mmol), tetrabutylammonium sulfate (0.45 g, 1.3 mmol), and potassium carbonate (18.2 g, 132 mmol) and stirred and refluxed under N_2 overnight. The solution was filtered and the residue was washed with hot $CHCl_3$ (2 × 30 mL). The organic solvent was removed under reduced pressure. The crude product was purified using flash silica and a 50:50 ethyl acetate−ether solution. Removal of the eluant by reduced pressure yielded the product as yellowish crystals (0.51 g, yield: 26.5%).

^1H NMR ($CDCl_3$) δ 8.45 (H_1), 7.65 ($H_{3'}$), 7.55 ($H_{5'}$), 6.35 ($H_{4'}$). ^{13}C NMR ($CDCl_3$): δ 141.8 ($C_{3'}$), 129.6 ($C_{5'}$), 107.3 ($C_{4'}$), 83.2 (C_1). ^{15}N NMR ($CDCl_3$): δ 303.4 ($N_{2'}$), 210.7 ($N_{1'}$). The ^{15}N and ^{13}C chemical shifts were referenced against liquid ammonia[45] and internal TMS, respectively.

Acknowledgment. Helpful discussions with Dr. P. E. Hansen and Dr. L. D. Field are acknowledged. G.O. thanks the Swedish Natural Research Council (Project 10161) and the Wallenberg foundation for financial support. B.A.M. and L.P.S. thank the Australian Research Council for support and the University of Sydney for a Gritton Scholarship.

JA9540177

(38) Shaka, A. J.; Barker, P. B.; Freeman, *J. Magn. Reson*. **1985**, *64*, 547−552.

(39) Boyd, J.; Soffe, N.; John, B.; Plant, D.; Hurd, R. *J. Magn. Reson.* **1992**, *98*, 660−664.

(40) Tolman, J. R.; Chung, J.; Prestegard, J. H. *J. Magn. Reson*. **1992**, *98*, 462−467.

(41) Ross, A.; Czisch, M.; Cieslar, C.; Holak, T. A. *J. Biomol. NMR* **1993**, *3*, 215−224.

(42) Emsley, L.; Bodenhausen, G. *Chem. Phys. Lett*. **1990**, *165*, 469−476.

(43) Protopova, T. V.; Skoldinov, A. P. *Zh. Obshchei Khim*. **1956**, *26*, 3733−3737.

(44) Julia, S.; del Mazo, J. M.; Avila, L.; Elguero, J. *Org. Prep., Proc. Int*. **1984**, *16*, 299−307.

(45) Live, D. H.; Davis, D. G.; Agosta, W. C.; Cowburn, D. *J. Am. Chem. Soc.* **1984**, *106*, 1939−1941.